Aliphatic Polyamidoamine Hyperbranched Polymers/ Layered Silicate Nanocomposites

A. Amin, A. S. Taha, M. A. Abd El-Ghaffar

Department of Polymers and Pigments, National Research Center, Dokki-Giza, Egypt

Received 29 October 2009; accepted 21 February 2010
DOI 10.1002/app.32361
Published online 21 May 2010 in Wiley InterScience (www.interscience.wiley.com).

ABSTRACT: Polyamidoamine hyperbranched polymer (Hyp)/clay nanocomposites were synthesized by using both of montmorillonite and laponite clays. Poly amidoamine hyperbranched polymer (Hyp) was prepared by one-pot polymerization via couple monomer methodology. Afterward, the amino ends of Hyp were modified with methyl methacrylate (MMA), styrene (St) and butyl methacrylate (*n*-BuMA) polymers which were previously prepared via ATRP (atom transfer radical polymerization) to form the corresponding new hyperbranched polymers Hyp_1, Hyp_2 and Hyp_3. Those formed polymers were inserted into the modified clay, such as montmorillonite and laponite to form their nanocomposites. The formed polymer/clay nanocomposites were characterized via XRD, TEM, and thermal analyses. The formed hyperbranched polymers generally showed intercalation behavior more than the exfoliation one mostly because of the bulkiness of the hyperbranched skeleton. © 2010 Wiley Periodicals, Inc. J Appl Polym Sci 118: 525–537, 2010

Key words: hyperbranched polymers; Laponite; montmorillonite; nanocomposites; ATRP

INTRODUCTION

Great attention was dedicated during the last decades for the introduction of nanofillers in polymeric matrices to improve a range of properties and accordingly broadening of the final uses of the resulting composites. Amongst nanofillers, layered aluminiosilicates such as montmorillonite and laponite, have been intensively studied. The produced nanocomposites may exhibit different morphologies; intercalated or at best semi-intercalated/semiexfoliated. They have a wide range of vital applications which have been driven by the potential to create new material systems with outstanding properties.[1–3] Accordingly, clays have been extensively used as reinforcing agents to prepare polymer-layered silicate nanocomposites.[4–8] Generally, Clay improves the polymer performance over conventional fillers with smaller loading content. Polymer/clay nanocomposites combine the advantages of both of clay such as rigidity, high stability and the organic polymers such as flexibility, dielectric, ductility and processibility. The advantages of nanocomposites include enhanced mechanical properties, thermal resistance and other improvements in barrier properties when compared with the pristine matrix.[9–11] The efficiency of clays to modify the properties of the polymer is primarily determined by the degree of its dispersion in the polymer matrix.[12] Morphology and structure are important factors governing the properties of nanocomposites.[13] Several polymers have been involved in the polymer/clay nanocomposites such as acrylates,[14–19] styrene,[20–24] 4-vinylpyridine,[25] acrylamides,[26] and poly-*N*-isopropylacrylamide.[27] Additionally, selective polymers have been used as poly(*N*-vinyl pyrrolidone),[28,29] poly(ethylene glycol),[30] polybenzoxazole,[31] polypropylene (PP),[32–34] and polyethylene (PE).[35] Recently, hyperbranched polymers[36] were successfully used in the preparation of the polymer-clay nanocomposites to invest their excellent chemical and physical properties to obtain composites with enhanced characteristics. The interest in hyperbranched polymers is growing rapidly due to their unique properties and potential applications in various fields from drug-delivery to coatings.[37–44] They are considered as relatively new class of highly active macromolecules.[45,46] Several methods can be used to synthesize hyperbranched polymers from non-iterative polymerization procedures, such as step-growth polycondensation, self-condensing vinyl polymerization and multibranching ring-opening polymerization.[47–53] Regardless of the method of preparation, the physical properties of the hyperbranched are of key importance with respect to their implementation in industrial applications in comparison to their linear analogs.[37–44] The large number of functional end groups attached to the hyperbranched polymers can be conveniently end-capped to produce novel functional polymeric

Correspondence to: A. Amin (aamin_07@yahoo.com).

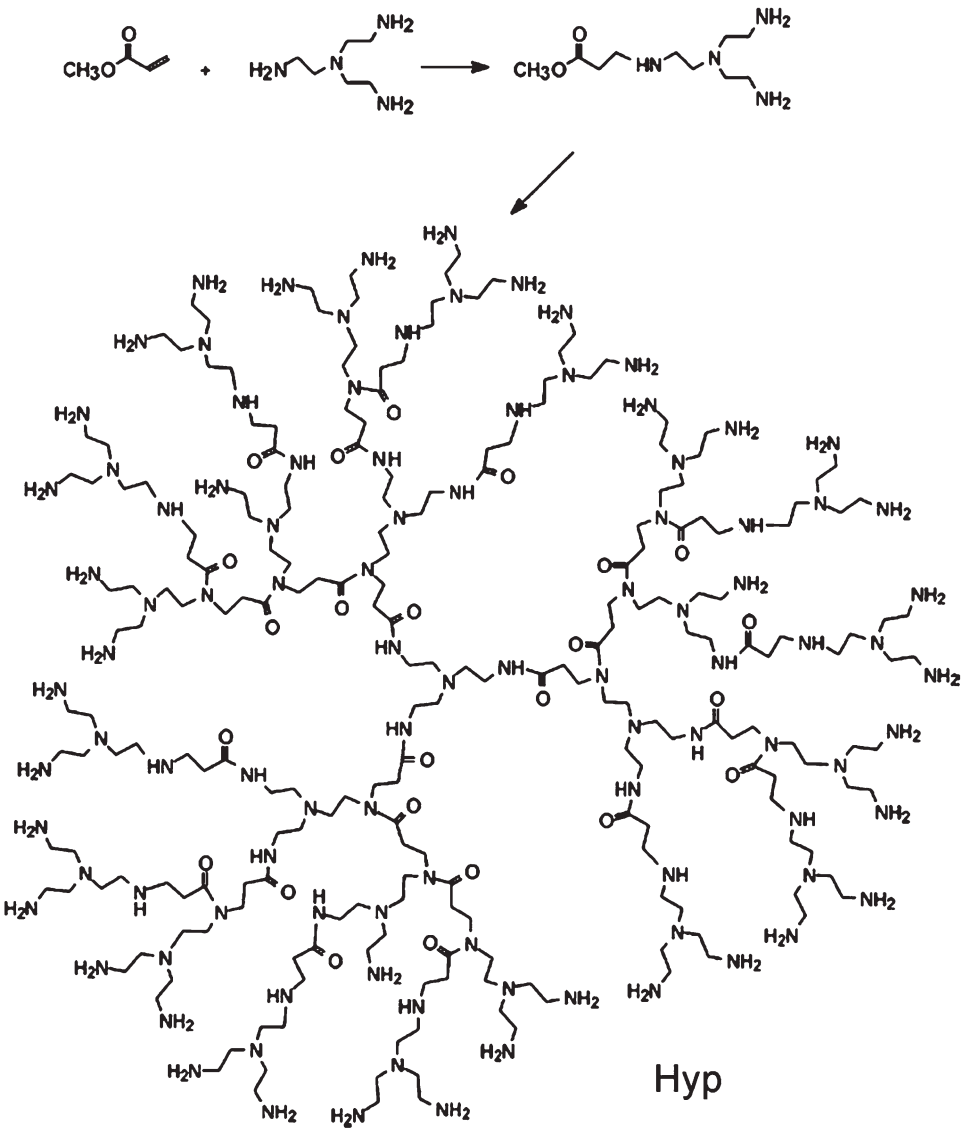

Scheme 1 Preparation of polyamidoamine hyperbranched polymer (Hyp).

materials with new properties. Therefore, herein, the hyperbranched ends were modified with well defined acrylates and styrene polymers that were prepared via atom transfer radical polymerization (ATRP). ATRP appeared at the last few years as the most widely used controlled polymerization techniques to provide polymers with well-known structures. Through ATRP, acrylates,[54] methacrylates,[55,56] and styrene[57] were polymerized and copolymerized. Several alkyl halides were used as initiators.[58] Also, *N*-based ligands were used in conjunction with CuBr as successful catalytic systems, such as 2,2′ bipyridine,[59] pyridinimines,[55] phenanthrolines,[60] and pentamethyldiethylenetriamine and the corresponding permethylatedtetramine.[61] Therefore, herein, the polyamide amine hyperbranched polymer (Hyp) was prepared as previously mentioned in the literature and as indicated in Scheme 1.[62] Then, Hyp with polar amino ends was inserted into clay to form intercalated polymer/clay nanocomposites. Also, trials to form nanocomposites from the salt of the hyperbranched polymer (Hyp) were carried out. In a subsequent step, the amino ends of the polyamidoamine hyperbranched polymers were modified with Br- ended polymers which were previously prepared via ATRP to form core-shell architecture from the terminal hydrophobic polymeric units and the polar amine-containing core. The core shell architecture is very important in several applications. Then, the resulting modified hyperbranched polymers were introduced into the modified clay which was first treated with low molecular weight organic compound, such as cetyltrimethyl ammonium bromide (CTAB). The total reactions pathway was represented as shown in Scheme 2.

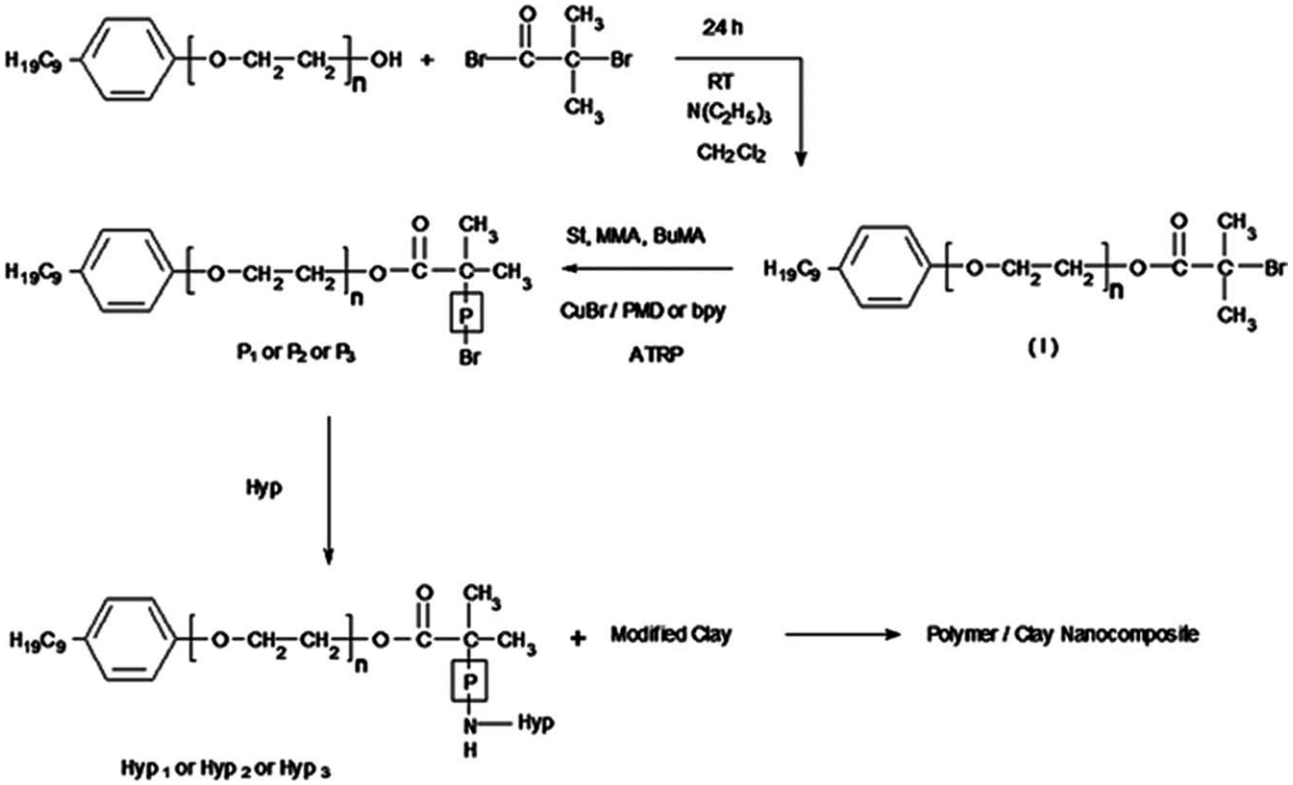

Scheme 2 Preparation of polymer/clay nanocomposite

EXPERIMENTAL

Chemicals

Tris-2-aminoethylamine, 2-bromoisobutyryl bromide, Cetyl trimethylammonium bromide (CTAB) and copper (I) bromide (CuBr) (99.99%) were supplied from Sigma-Aldrich Chemical Company (USA). Pentamethyldiethylene triamine (PMD) and bipyridine (bpy) were from PARK Scientific Limited Chemicals-Northampton- UK. All other general reagents and solvents were of commercial grades from Sisco Research Laboratories (SRL) (India). Surfactant such as Tergitol–NP50, $M_w = 700$, $[C_{19}H_9C_6H_4(OCH_2CH_2)_xOH]$ was provided from Modern Lab. (Egypt). Montmorillonite (MMT) and Laponite (Lap) clays were provided by Southern Clay Products, Texas. Several monomers were used such as Methyl methacrylate (MMA), styrene (St.), *n*-butyl methacrylate (*n*-BuMA) and methyl acrylate (MA). All monomers were received from Merck Chemical Company (Germany). They were purified by filtration through an activated basic alumina column then stored under argon in the freezer.

Instrumentations

Gel permeation chromatography (GPC) was used to determine both of the Molecular weights ($\overline{M}_{nGPC}$) and the polydispersities (PDI) of the prepared polymers by using GPC-1100 Agilent technologies with refractive index detector with 100-10^4-10^5 A^o ultrastyragel columns connected in series. THF and DMF were used as the eluents with flow rate 1 mL min$^{-1.}$ Commercially available linear polystyrene standards were used to calibrate the columns. Nuclear magnetic resonance (^{1}H-NMR) spectra were recorded on Varian Mercury-Oxford-300 MZ where tetramethylsilane TMS was used as internal standard. Also, $CDCl_3$ and DMSO were used as solvents. IR spectra were recorded on Bruker IR IFS 113 V, by using KBr pellets. X-ray diffraction (XRD) was widely employed for characterization of nanocomposites by measuring the basal spaces (d) between the layers of clay. Measurements were acquired with Brukur D8 Advance operating at 60 kV and 40 mA. The X-ray is emitted by a source (Co – CuK_α target with secondary monochromator). Transmission electron microscopy (TEM) measurements were acquired with JEM – 1230 – electron microscopy operated at 60 kV. Samples were prepared by drop casting the suspension of the polymers onto carbon-coated copper grids, followed by evaporation of the solvent in air. Fine and nanostructures were expected for the prepared polymer-clay nanocomposites. Both of thermal gravimetric analysis (TGA) and differential scanning calorimetry (DSC) were carried out on NETZSCH STA 409 -DSC differential scanning calorimeter by using sample weight of 50 mg under nitrogen atmosphere.

Synthetic procedures

Preparation of polyamidoamine hyperbranched polymer (Hyp)

As shown in Scheme 1, Hyp was prepared as previously described in the literature[62] and as the following:

(0.901 mL, 0.01 mol) of Methyl acrylate monomer (MA) was added drop-wise to (1.497 mL, 0.01 mol) of tris-2-aminoethylamine in 100 mL of methanol. The reaction mixture was kept at room temperature for 24–48 h. Then, the solvent was removed from the reaction mixture under reduced pressure at 60°C. Under vigorous revolving and vacuum distillation, the mixture was kept at 60°C for 1 h, 100°C for 2 h, 120°C for 2–4 h, and finally 135–150 °C for other 2–4 h. Pale yellow viscous hyperbranched polymer was produced. The yield was $\geq$ 95%. Further characterization was carried out for the prepared Hyp by GPC, IR and ^{1}H-NMR. GPC (PS): (M_n = 32,094 g/mol). IR (KBr)-stretching: ν (NH_2): 3286, 3388 cm^{-1}. ν (NH): 3090 cm^{-1}, ν (CH_3, CH_2): 2941, 2843 cm^{-1}. ν (CO): 1650 cm^{-1}, ν (CN): 1555 cm^{-1}. ^{1}H-NMR ($CDCl_3$):δ= 2.41 ppm (NH_2), 2.51–2.70 ppm ($COCH_2$, $NHCH_2$, NH_2 CH_2), 3.12–3.54 ppm (NCH_2).

Preparation of Hyp salt

A solution of hyperbranched polymer (Hyp, M.wt= 32,094 gm/mol, 1.5 gm, × 10^{-5} 4.72 × 10^{-5} mol) in 50 mL ethyl acetate was acidified to pH = 4 by drop-wise addition of conc. HCl at RT for 30 min. The solvent was removed under reduced pressure then the residue was extracted with diethylether and dried under vacuum to afford hydrochloride salt.

Preparation of polyamidoamine hyperbranched polymer (Hyp)/clay nanocomposites

0.45 gm and 0.12 gm for unmodified MMT or Lap representing 15 wt % and 4 wt % clay loading contents, respectively, were dispersed in 60 mL distilled H_2O for 24 h at 60°C. 3 gm, 9.35 × 10^{-5} mol of Hyp were dissolved in 40 mL distilled H_2O for 3 h at the same temperature. Hyp solution was added to the dispersed clay and stirred for 24 h at 60°C. The formed precipitate was filtered and washed by distilled water several times then the product was dried and ground to form fine powder. The salt of the hyperbranched polymer was inserted inside the clay by similar methodology as in case of the normal hyperbranched polymer (Hyp). The formed nanocomposites were characterized by XRD, TEM and thermal analyses.

Modification of the hyperbranched ends

The end groups of the formed Hyp were modified by some functional polymers which were prepared via ATRP. The ATRP polymers with Br-ends easily reacted with the amino ends of the original hyperbranched polymer. ATRP polymerization processes were carried out for MMA, St and *n*-BuMA monomers as will be described in the following:

Preparation of ATRP initiator (I). 0.7 gm (0.001 mol) of Surfactant (Tergitol-NP_{50}, M.wt = 700) was placed in three-necked round-bottom flask and dissolved in 150 mL of anhydrous CH_2Cl_2. Then, 0.279 mL, 0.002 mol of triethylamine was successively added with continuous stirring. 0.247 mL, 0.002 mol of 2-bromoisobutyryl bromide was added drop-wise to the reaction mixture. The reaction was left for 24–27 h to completion at room temperature. The resulting solution was extracted by using distilled water several times then the obtained solution was dried with anhydrous Na_2SO_4. The solution was filtered and the solvent was evaporated in vacuo. The product was characterized by using ^{1}H-NMR and IR. ^{1}H-NMR ($CDCl_3$):δ = 1.5–1.827 ppm (CH_3), 2–2.2 ppm (CH_2, C_9H_{19}), 3.5–4.2 ppm (OCH_2CH_2), 6.4–7.2 ppm (ph, H). IR (KBr) stretching: ν (C=O): 1750 cm^{-1}, ν (C-H of CH_3, CH_2, and CH, aliphatic): 2770- 2990 cm^{-1} (broad band), ν (C-H, aromatic): 3470 cm^{-1}.

Preparation of MMA, st and n-*BuMA homopolymers via ATRP.* To a glass vial, under argon atmosphere, the proper amounts of CuBr (0.144 gm, 1 × 10^{-3} mol), ligand (15 × 10^{-4} mol = 0.313 gm and 0.234 gm for PMD and bpy, respectively), toluene and monomers such as MMA, St and *n*-BuMA were successively added. The monomer amounts were calculated with molar ratio 100 times with respect to the initiator. The vial was immersed in an oil bath with stirring at 90°C. Then, 0.849 gm, 1 × 10^{-3} mol of the initiator (I) in 2 mL of solvent was added to the reaction mixture. Generally, the reactants were added in molar ratios (ligand: CuBr: initiator: monomer = 1.5: 1: 1: 100). Bpy was the proper ligand for ATRP of MMA and *n*-BuMA. However, PMD was the best ligand for St. After definite time intervals, the formed polymer was dissolved in THF and passed through alumina column to remove the metal residues. Then, the pure polymer solution was precipitated in *n*-hexane where the resulting polymer was characterized by GPC and ^{1}H-NMR. The total reactions were represented as shown in Scheme 2 where p refers to different polymeric ends such as P_1, P_2 and P_3 corresponding to MMA, St and *n*-BuMA ends, respectively. $\overline{M}_{nGPC}$ (PS) for P_1, P_2 and P_3 = 5407, 25,678 and 10,696 g/ mol where PDI= 1.17, 1.4 and 1.19, respectively. ^{1}H-NMR of MMA polymers indicated that δ = 1.36–1.86 ppm (CH_3), 3.6 ppm (OCH_3) and 3.8–4.2 ppm (OCH_2CH_2). However for St, dense bands appeared in high intensity at 6.2-7.4 ppm which were referred to the phenyl groups inside the skeleton of the polymer. In case of *n*-BuMA, additional bands appeared at 4.1 ppm referring to CH_2

TABLE I
Trials of Formation of Hyp/Clay Nanocomposites

Entry	Conditions	*d* (XRD) nm	Entry	Conditions	*d* (XRD) nm
A_1	MMT	1.226	$\overline{A}_8$	MMT-CTAB + Hyp_1 (4%MMT)	3.088
$\underline{A}_2$	Hyp (15% MMT)	1.397	$\underline{A}_9$	MMT-CTAB + Hyp_2 (15%MMT)	1.507
$\overline{A}_2$	Hyp (4% MMT)	1.705	$\overline{A}_9$	MMT-CTAB + Hyp_2 (4% MMT)	1.618
$\underline{A}_3$	Quaternized Hyp (15% MMT)	1.361	$\underline{A}_{10}$	MMT-CTAB + Hyp_3 (15%MMT)	1.575
$\overline{A}_3$	Quaternized Hyp (4% MMT)	Exfoliated	$\overline{A}_{10}$	MMT-CTAB + Hyp_3 (4% MMT)	1.696
A_4	Untreated Lap	1.249	A_{11}	Lap-CTAB	1.842
$\underline{A}_5$	Hyp (15% Lap)	1.410	$\underline{A}_{12}$	Lap-CTAB + Hyp_1 (15% Lap)	1.495
$\overline{A}_5$	Hyp (4% Lap)	2.193	$\overline{A}_{12}$	Lap-CTAB + Hyp_1 (4% MMT)	1.729
$\underline{A}_6$	Quaternized Hyp (15% Lap)	1.266	$\underline{A}_{13}$	Lap-CTAB + Hyp_2 (15% Lap)	1.643
$\overline{A}_6$	Quaternized Hyp (4% Lap)	Exfoliated	$\overline{A}_{13}$	Lap-CTAB + Hyp_2 (4% MMT)	1.745
A_7	MMT-CTAB	1.839	$\underline{A}_{14}$	Lap-CTAB + Hyp_3 (15% Lap)	1.962
A_8	MMT-CTAB + Hyp_1 (15%MMT)	1.554	$\overline{A}_{14}$	Lap-CTAB + Hyp_3 (4% MMT)	2.065

groups in COO $(CH_2)_3CH_3$ of the side chain of the butyl moiety.

Preparation of MMA, St, n-*BuMA modified hyperbranched polymers.* As shown in Scheme 2, hyperbranched polymer (Hyp) was modified by polymeric ends. Hereby, (3.209 gm, 0.0001 mol) of the principle polymer (Hyp) were introduced into three-necked round-bottom flask and dissolved in 50 mL anhydrous CH_2Cl_2. Triethylamine (0.02 mL, 15×10^{-5} mol) was successively added with continuous stirring. Then, Br-ended polymer (P_1, P_2 or P_3, 1×10^{-4} mol according to each polymer), was dissolved in 50 mL anhydrous CH_2Cl_2 and added drop-wise to the reaction mixture. The reaction was left for 24–27 h at room temperature. The resulting solution in each case was extracted by using distilled water several times (~ 50 mL/3 times). The obtained solution was dried with anhydrous Na_2SO_4, then filtered and the solvent was evaporated in vacuo. The modified hyperbranched polymers Hyp_1, Hyp_2, and Hyp_3 were obtained corresponding to the originally reacted polymeric ends (e.g. P_1, P_2, and P_3). The formed modified hyperbranched polymers were characterized via GPC and ^{1}H-NMR where $\overline{M}_{nGPC}$ values for Hyp_1, Hyp_2, and Hyp_3 were 29,677, 51,932 and 50,892 g/mol, respectively. Also, ^{1}H-NMR confirmed the structures of the formed polymers as previously described with respect to the individual polymers P_1, P_2 and P_3. The modified polyamidoamine hyperbranched polymers with the new hydrophobic polymeric ends were inserted into clay after modification of such clay (MMT or Lap) with cetyltrimethyl ammonium bromide (CTAB).

Modification of clay

20 gm of clay (montmorillonite or laponite) were dispersed in 500 mL distilled water containing 6 gm, 65×10^{-4} mol of CTAB, which caused complete cation exchange, at room temperature then the temperature was increased to 80°C under vigorous stirring for 6–8 h. The resulting modified clay was separated by filtration and washed several times with distilled water. The resulting modified clay was vacuum dried at 60°C for 24 h. MMT-CTAB and Lap-CTAB refer to the treated montmorillonite and laponite with CTAB. The prepared organo-modified clay (MMT-CTAB and Lap-CTAB) were characterized via XRD.

Preparation of modified hyperbranched polymers/clay nanocomposites

The prepared hyperbranched polymer (i.e. Hyp_1, Hyp_2, Hyp_3, ~3 gm) in each case was dissolved in 40 mL distilled water at 60°C with stirring for 3 h then 20 mL of DMF were added to facilitate the total solubility of the modified hyperbranched polymer. Then, the resulting solution was added to 60 mL dispersed phase of MMT-CTAB or Lap-CTAB (e.g. 0.45 gm, 15% and 0.12 gm, 4 %) with stirring at 60°C for 24 h. The formed nanocomposite was separated by filtration and washed several times with distilled water before drying at vacuum at 60°C for 24 h. The formed nanocomposites were characterized by XRD, TEM and thermal analyses.

RESULTS & DISCUSSION

Preparation of polyamidoamine hyperbranched polymer (Hyp)/clay nanocomposites

The polyamidoamine hyperbranched polymer (Hyp) was prepared via one pot reaction of methyl acrylate (MA) and tris-2-aminoethylamine.[62] The structure of the formed hyperbranched polymer which is illustrated in Scheme 1 was proved in terms of GPC, IR and ^{1}H-NMR as was mentioned before. Some experiments were conducted to insert Hyp into unmodified clay such as montmorillonite (MMT) and laponite (Lap) in different clay loading contents (15 wt %, 4 wt %) as shown in Table I. Since the prepared polymers were of reasonable polarity with high

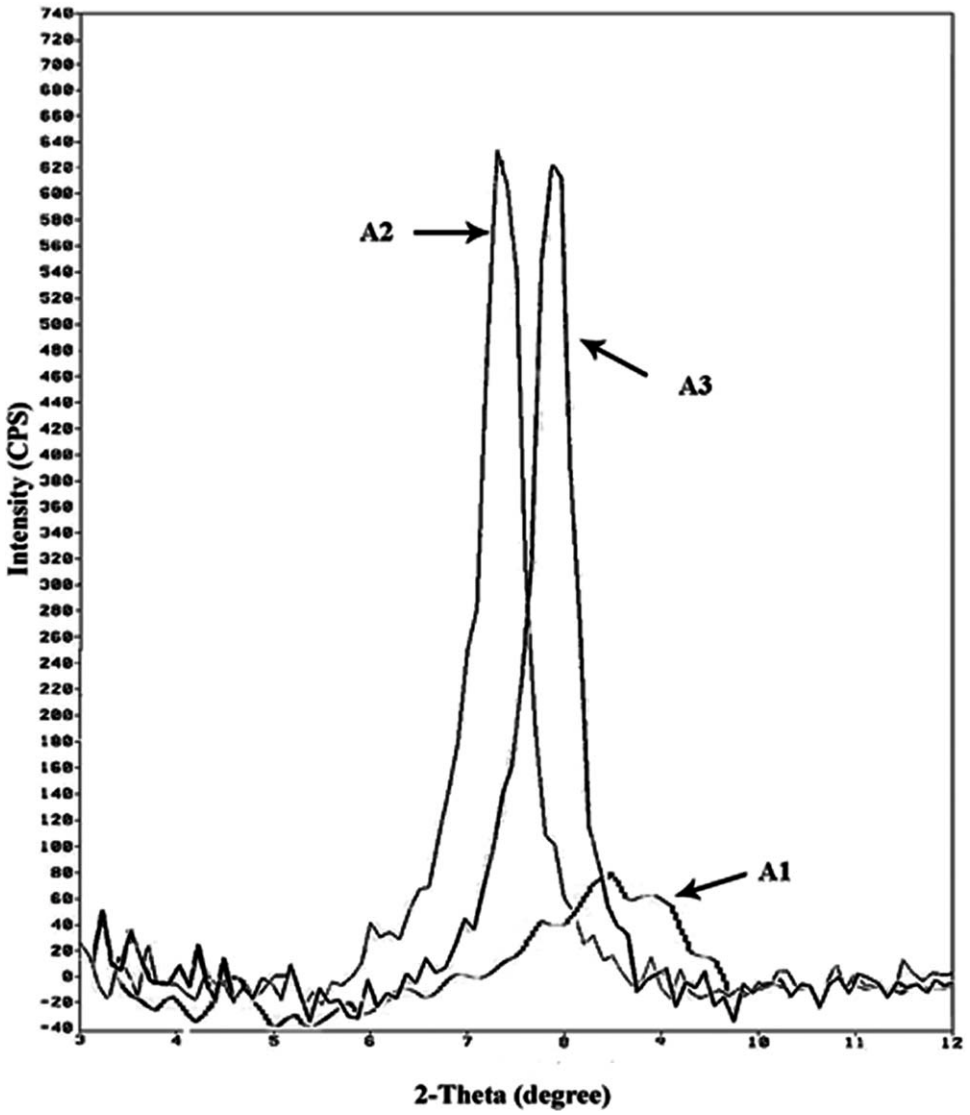

Figure 1 XRD of A_1, A_2, and A_3.

content of polar terminals such as amino groups, these types of polymers were firstly inserted into the interlayer space of clay particles directly without pretreatment for clay. The formed Hyp/ clay nanocomposites were characterized via XRD.

Hyp- MMT and quaternized- Hyp- MMT nanocomposites

Firstly, XRD of montmorillonite clay itself, (A_1) as in Figure 1, revealed the appearance of a diffraction sharp peak around 2 theta 8.5 which was indicative of regular repetitions of silicate layers. The distance between a layer and the following corresponding one was estimated to be 1.226 nm. Then, trials to insert Hyp- polymer were carried out for intercalation onto the pristine clay from aqueous medium as in case of A_2, $\overline{A}_2$ with different clay loading contents. As shown in Figures 1 and 2, the basal space enlarged to 1.397 nm at lower intensity and became sharper than A_1 at 15% clay content for A_2 which increased to 1.705 nm at 4% clay with respect to $\overline{A}_2$. These results proved that the clay layers became

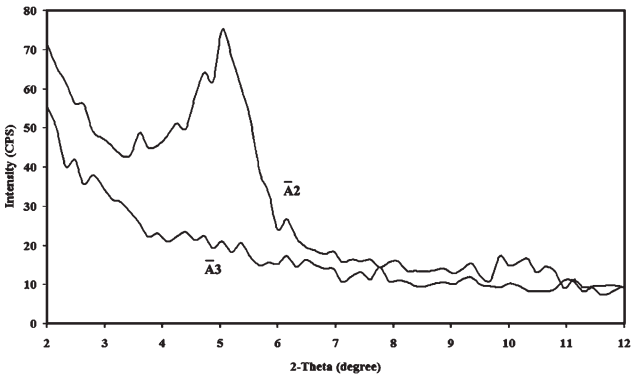

Figure 2 XRD of $\overline{A}_2$ and $\overline{A}_3$.

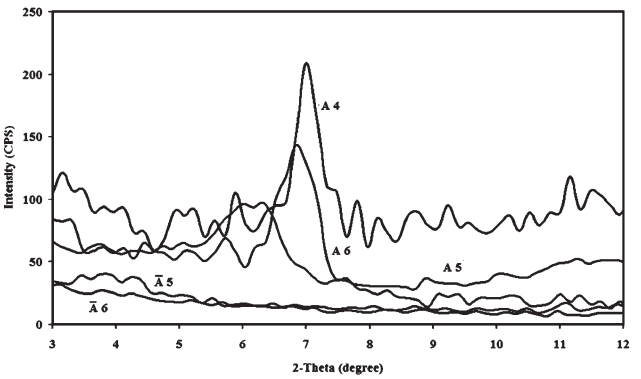

Figure 3 XRD of A_4, A_5, $\overline{A}_5$, A_6, and $\overline{A}_6$.

well and regularly ordered with intercalated structure upon processing with a higher polymer in the form of masterbatch. Other trials were performed to insert the quaternized form of the polyamidoamine hyperbranched polymers into the unmodified clay (i.e. A_3, $\overline{A}_3$). With respect to A_3, (Fig. 1), a sharp band with comparable intensity was obtained at 15% clay which gave rise to a comparable basal space (1.361 nm). Here, most of the basic centers with the NH_2 functionalities in Hyp acquired the quaternized positively charged form which meant that their intercalation mode onto the clay interlayer space was preferably performed by cation exchange rather than via polar- polar interaction. This additionally highlighted the role of the condensed repulsive forces induced by the positive charged species in tightening the basal space at higher clay loading content (15 %). However, complete exfoliation was obtained with respect to $\overline{A}_3$ (Fig. 2) at lower loading content of clay (4%), indicating complete destruction of the clay layers. Also, this answered the question that this process is a function of many tunable parameters mainly the nature of the hyperbranched structure, also whether quaternized or not, the degree of quaternization of such polymer, the applied volume of it with respect to the clay and the percentage of the used clay. It seemed that the temperature did not play any role with this respect up to the investigated range (60°C). Another nanofiller was investigated such as laponite, which is very similar in its chemistry to montmorillonite. However, its platelets width is of the order 25 nm while that of montmorillonite is up to 4 times as high as laponite (100 nm) while the thickness of one platelet is the same (1 nm) in both cases. The basal space for A_4 (Fig. 3) was determined to be 1.249 nm.

Hyp-lap and quaternized Hyp-lap nanocomposites

Some experiments were carried out to insert Hyp into Laponite to form polymer/clay nanocomposites as indicated in Table I. The basal space of A_5 as illustrated in Figure 3 increased to 1.4103 for 15% clay content with more broadening at lower intensity which proved that the clay layers formed obvious intercalated nanocomposites. Also, the basal space increased to 2.193 nm by decreasing the clay content to 4% for $\overline{A}_5$ causing more efficient intercalation. The treatment of clay with *in situ* protonated hyperbranched polymer (A_6, Fig. 3) did not reveal any extra expansion at 15% clay where basal space recorded 1.266 nm. However, some broadening was noticed for different peaks which may be attributed to incomplete quaternization of NH_2 centers or the higher degree of branching in such hyperbranched polymer. This point of great importance, however it needs further investigation. Surprisingly, by decreasing the clay loading content to 4%, $\overline{A}_6$, complete exfoliation happened as in Figure 3.

Preparation of modified hyperbranched polymers

A set of hydrophobic hyperbranched polymers were prepared as illustrated in Scheme 2 by reaction of the Br- terminated MMA, St and *n*-BuMA polymers (i.e. P_1, P_2, P_3), which were preformed via ATRP polymerization technique, with the NH_2- terminated parent hyperbranched polymer (Hyp) to produce special corresponding amphiphilic type of polymers with core-shell structure such as Hyp_1, Hyp_2 and Hyp_3, respectively. The ATRP initiator (I) was initially prepared by treating the surfactant (Tergitol- Np 50) with 2-bromoisobutyryl bromide in presence of triethylamine. The structure of the resulting I was confirmed by IR and ^{1}H-NMR as previously mentioned. The Br-ended polymeric surfactant (I) was used as macroinitiator to form the Br-ended polymers (i.e. P_1, P_2 and P_3) via ATRP of MMA, St and *n*-BuMA, respectively by using PMD and bpy ligands. The resulting polymers P_1, P_2 or P_3 were characterized by GPC and ^{1}H-NMR as described in the experimental section.

Preparation of modified hyperbranched polymers/clay nanocomposites

The previously modified hyperbranched polymers Hyp_1, Hyp_2 and Hyp_3 were inserted in the modified

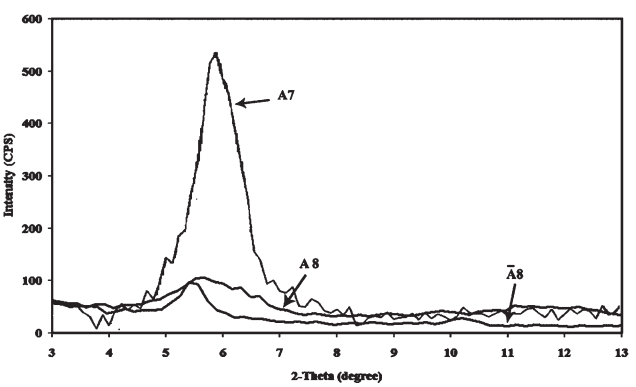

Figure 4 XRD of A_7, A_8, and $\overline{A}_8$.

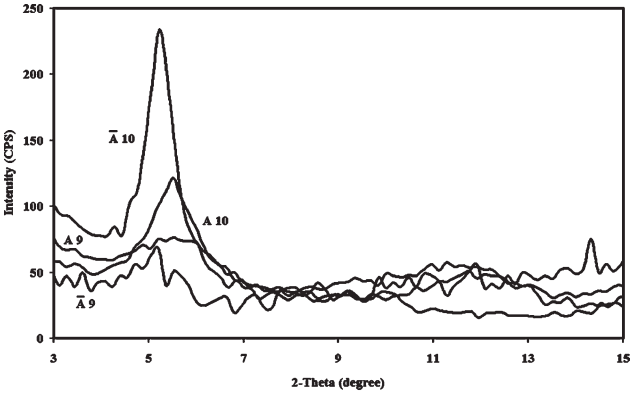

Figure 5 XRD of A_9, $\overline{A}_9$, A_{10}, and $\overline{A}_{10}$.

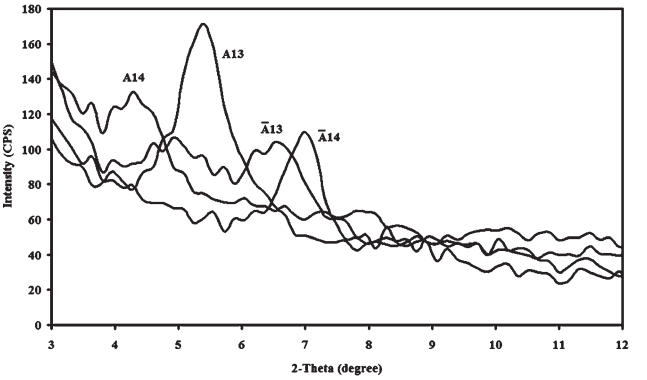

Figure 7 XRD of A_{13} and $\overline{A}_{13}$, A_{14}, and $\overline{A}_{14}$.

clay such as MMT-CTAB and Lap-CTAB as indicated in Table I. Generally, the resulting nanocomposites were characterized via XRD.

Modified hyperbranched polymers-MMT-CTAB nanocomposites

XRD of MMT-CTAB indicated that the basal space extended to 1.839 nm (A_7, Fig. 4) in comparison with the pristine clay (i.e., A_1, 1.226 nm). It was observed that the diffraction peak shifted backward where the peak intensity heightened which was a strong indication of a better ordering or stacking of CTAB molecules within the basal space of the silicate layers. Generally, the dual role of the treating agents such as CTAB is usually not only limited to their expanding action but extends also to their hydrophobizing power which qualifies them for incorporation into hydrophobic polymers in a subsequent stage during processing. Hence, the hydrophobic termini are so very compatible to spontaneously bind the hydrophobic clay moieties, with their platelets bearing long hydrocarbon tails, by hydrophobic-hydrophobic interactions. Also, it may be expected that the associated high repulsive forces between the crowded charged species can not come over the electrostatic attraction forces between the negatively charged clay platelets and the polymers and also the random distribution of the positive charges. That may account for the very small and modest expansion of the basal spaces where generally the hyperbranched polymers are well known to acquire very low hydrodynamic radii relative to their real volume which can so simply embed within the basal space of the montmorillonite or laponite. Accordingly, the basal spaces decreased to 1.554 nm in case of A_8 (Fig. 4) with MMA polymeric ends with lower intensity in diffraction peak at 15% clay content. The same situation was observed in case of A_9 (Fig. 5) with St ends and A_{10} with *n*-BuMA ends where the basal spaces decreased to 1.5073 nm and 1.5754 nm, respectively with lower intensities of the diffraction peaks than that observed in the original MMT-CTAB. However, the bulkiness of the polystyrene segments shell might be responsible for the low intensity of the diffraction peak. As illustrated in Table I, the basal space obviously increased by decreasing clay content to 4% incase of Hyp_1, Hyp_2 and Hyp_3/MMT-CTAB clay nanocomposites. Hereby, the basal spacing increased from 1.554, 1.507, 1.575 nm (A_8, A_9, A_{10}) to 3.088, 1.618, 1.696 nm ($\overline{A}_8$, $\overline{A}_9$, $\overline{A}_{10}$) at lower intensities. Those findings effectively

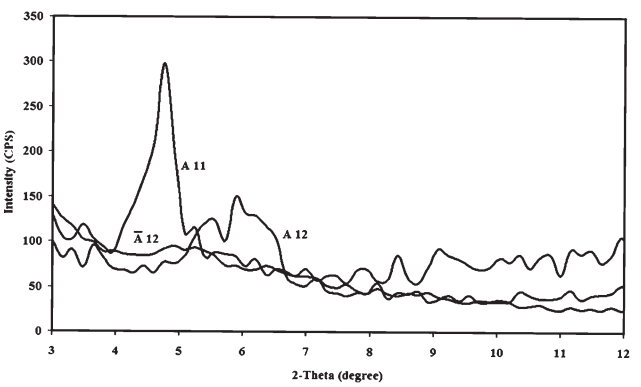

Figure 6 XRD of A_{11}, A_{12}, and $\overline{A}_{12}$.

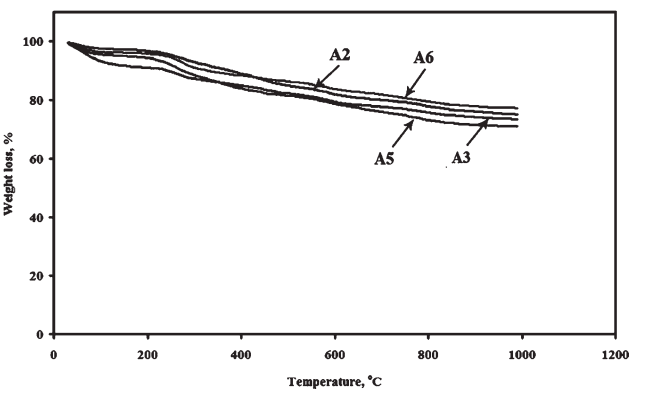

Figure 8 TGA of A_2, A_3, A_5, and A_6.

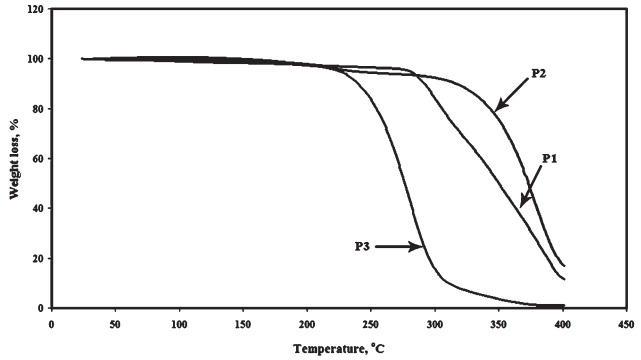

Figure 9 TGA of P_1, P_2, and P_3.

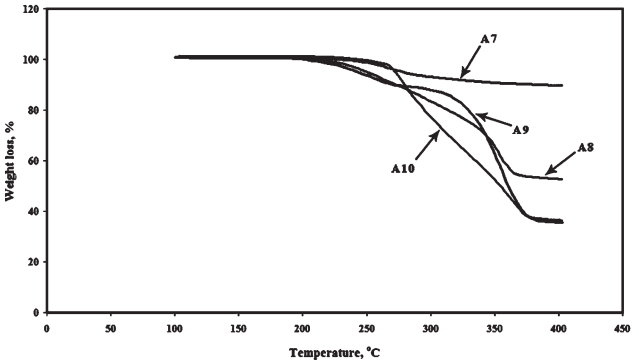

Figure 11 TGA of A_7, A_8, A_9, and A_{10}.

supported the formation of intercalated polymer/clay nanocomposites.

Modified hyperbranched polymers-Lap-CTAB nanocomposites

Laponite clay was also modified by using CTAB to form lap-CTAB (A_{11}). XRD of A_{11} (Fig. 6) acquired different peaks corresponding to basal space of 1.842 nm, which revealed 0.59 nm expansion than that in the original clay (i.e. Lap, A_4 = 1.249 nm). Some other trials were performed to insert the modified hyperbranched polymers (Hyp_1, Hyp_2, Hyp_3) inside Lap-CTAB as incase of MMT-CTAB as summarized in Table I. The layers of clay after modification became more qualified to be further intercalated with Hyp_1, Hyp_2 and Hyp_3 with high molecular weights. The formed polymer/clay nanocomposites in each case were characterized via XRD as indicated in Table I. Herein, Hyp_1, Hyp_2 and Hyp_3 have core-shell amphiphilic structure based on the polar hyperbranched-NH_2 terminated polymer in the core with MMA, St and *n*-BuMA chains in the shell. Interestingly, the basal space of A_{12} and $\overline{A}_{12}$ (Fig. 6), which refer to Hyp_1 with MMA ends with 15% and 4% clay contents, collapsed to 1.495 nm and 1.729 nm, respectively which accounted for the hyperbranched structures which usually acquire very small volume with respect to the normal linear polymers of comparable molecular weights so tightening of the layers was expected in such cases. However, the diffraction peaks mostly were of diminished intensities and broadening. Thus, the layers were no longer ordered; on the contrary, they became semi-destructed. The PMMA terminals were thought to act as the binding sites with the CTAB via hydrophobic-hydrophobic interactions while the polar termini with their repulsive forces were directed towards the aqueous phase. The same situation was obtained upon substituting the PMMA terminals with either St or *n*-BuMA chains, giving raise to low-intensity diffraction peaks with basal spaces in the order of 1.643 nm and 1.962 nm, respectively, forming the polymer/clay nanocomposites (A_{13} and A_{14} at 15% clay, Fig. 7) which illustrated the semi-exfoliative role of these core-shell amphiphiles. Those facts were supported by using 4% clay content where the basal spacing recorded 1.745 nm and 2.065 nm, respectively for $\overline{A}_{13}$ and $\overline{A}_{14}$ at low intensities. The previous results indicated efficient intercalated modified hyperbranched polymers/Lap-CTAB nanocomposites.

Thermal analyses of hyperbranched polymers/clay nanocomposites

Some of the prepared hyperbranched polymers/clay nanocomposites were characterized by thermal analyses via TGA and DSC. TGA thermograms of

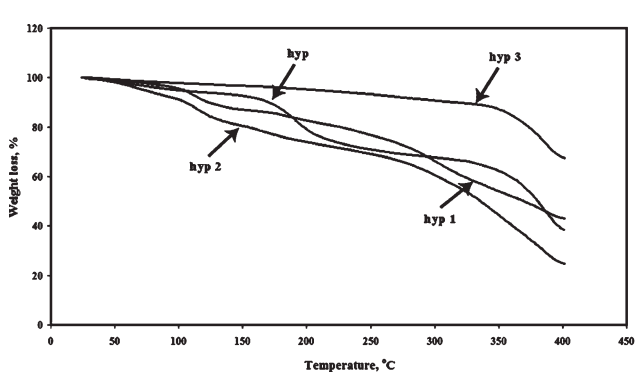

Figure 10 TGA of hyp, hyp_1, hyp_2, and hyp_3.

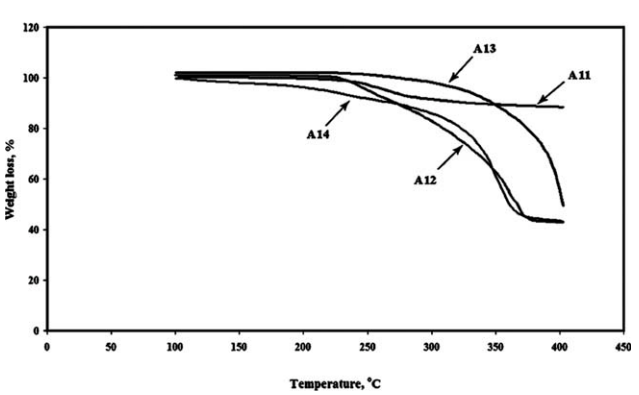

Figure 12 TGA of A_{11}, A_{12}, A_{13}, and A_{14}.

TABLE II
DSC Results of Hyp and Hyp/Clay Nanocomposites

Entry	Conditions	DSC (°C)	Entry	Conditions	DSC (°C)
A_2	Hyp (15% MMT)	105	A_7	MMT-CTAB	221.9
A_3	Quaternized Hyp (15% MMT)	106	A_8	MMT-CTAB + Hyp_1 (15%MMT)	245
A_5	Hyp (15% Lap)	95	A_9	MMT-CTAB + Hyp_2 (15%MMT)	253
A_6	Quaternized Hyp (15% Lap)	123	A_{10}	MMT-CTAB + Hyp_3 (15%MMT)	255
Hyp	original hyper-branched polymer	6	A_{11}	Lap-CTAB	207.8
Hyp_1	Hyp- MMA	60	A_{12}	Lap-CTAB + Hyp_1 (15% Lap)	153
Hyp_2	Hyp- St	47	A_{13}	Lap-CTAB + Hyp_2 (15% Lap)	99
Hyp_3	Hyp-*n*-BuMA	45	A_{14}	Lap-CTAB + Hyp_3 (15% Lap)	120

A_2, A_3, A_5, and A_6 nanocomposites (Fig. 8) indicated weight loss, such as 25, 27, 29, and 23%, respectively till 1000°C. The TGA thermograms of P_1, P_2 and P_3 polymers (Fig. 9) indicated a slight weight loss (3%, 6.6% and 10%) up to 280°C for both P_1 and P_2 and up to 250°C for P_3 which may be due to bounded water. Then, sharp loss started up to 400°C (i.e., 88%, 77.4% for P_1, P_2 and 89% for P_3) indicating complete decomposition of those polymers. TGA thermograms of Hyp, Hyp_1, Hyp_2, Hyp_3 were shown in Figure 10. Hyp lost 8% of its initial mass up to 160°C and extra loss (4.33%) up to 180°C which may correspond to bounded water, this was followed by other gradual loss of about 20% from 160 to 235°C and about 8.3% loss from 235 to 343°C which was attributed to the decomposition of the amino end groups of the Hyp polymer. Hyp polymer retained about 40% of its initial mass at 400°C. Hyp_1 lost 11.9% from its initial mass up to 140°C which was ascribed to bounded water but it retained 40% of its initial mass at 400°C. The 60% loss of its initial mass may be due to gradual decomposition of the amino end groups and decarboxylation of the ester and the amide linkages of the polymer. Hyp_2 lost 10% of its initial weight till 105°C then it decomposed where only 25% of its initial mass was left till 400°C. On contrary, Hyp_3 lost only 10% of its weight till 317°C and it retained 67.59% of its initial mass till 400°C. The heat stability of the modified hyperbranched polymers can be arranged in the following descending order (Hyp_3>>Hyp_1>>Hyp_2) which refers to the stability of aliphatic polymers than the aromatic ones which can be interpreted to the steric hindrance of aromatic hyperbranched polymers than the aliphatic ones. Slight weight loss of 10% was observed with respect to A_7, A_8, A_9 and A_{10} till 250°C (Fig. 11), then gradual decomposition was observed for A_8, A_9, and A_{10} till 450°C, on contrary to A_7 which stayed stable to the same degree. As illustrated in Figure 12, A_{11}, A_{12}, A_{13}, A_{14} began to decompose at 200°C where gradual decomposition was observed till 400°C.

The glass transition temperatures (T_g) of the previous samples were measured by DSC as illustrated in Table II. Some shifts in the T_g values were found in case of Hyp_1, Hyp_2, and Hyp_3 with respect to the original hyperbranched polymer (Hyp) according to the type and the chemical structure of the introduced polymer to the Hyp skeleton.

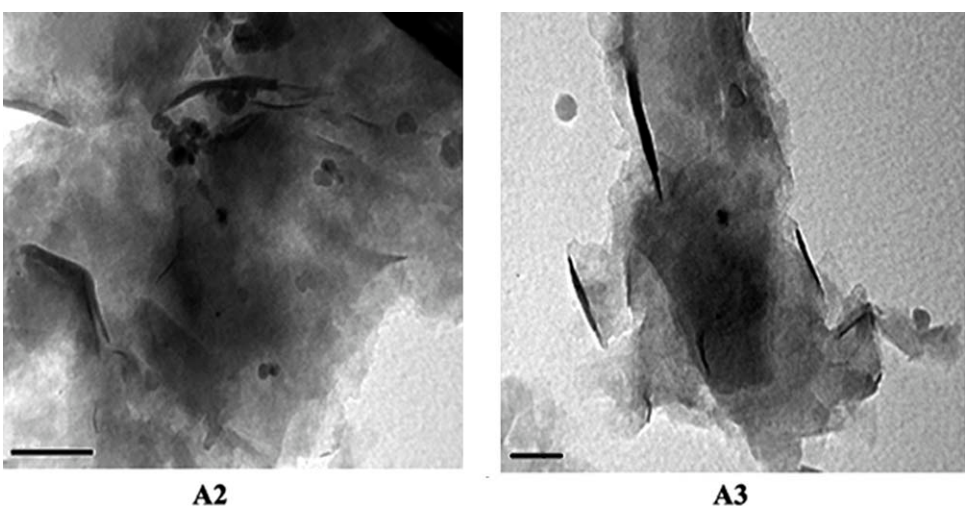

Figure 13 TEM of A_2 and A_3 (black bar = 200 nm).

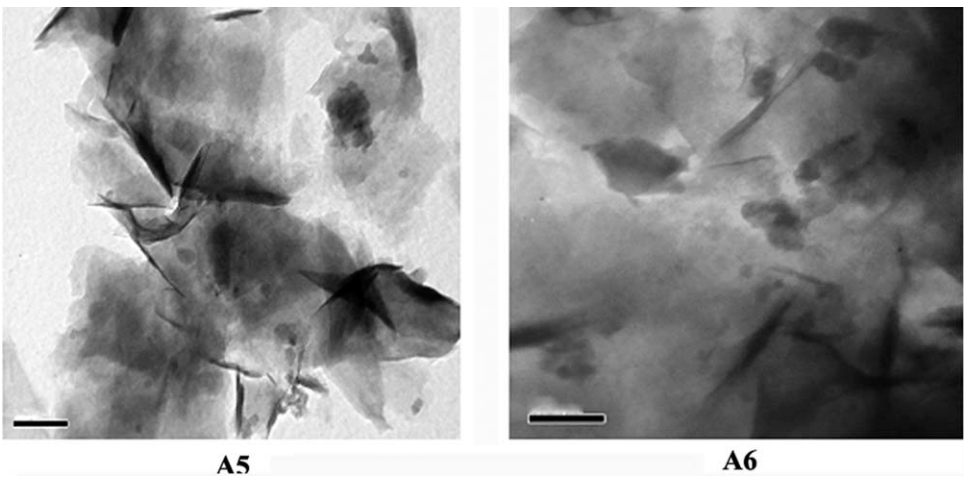

Figure 14 TEM of A_5 and A_6 (black bar = 200 nm).

TEM of hyperbranched polymers/clay nanocomposites

Some of the prepared nanocomposites were characterized by TEM as illustrated in Figures (13–16). Figure 13 shows intercalated nanocomposites with polymer matrices as in case of A_2 and A_3 where the clay tactoids exist in both cases. The same situation was observed as in case of A_5 and A_6 (Fig. 14). Figure 15 illustrates TEM micrographs of A_8, A_9, and A_{10}. It is clearly seen by analyzing TEM images that intercalated platelets are present in the polymer matrices showing good and uniform distribution of the MMT

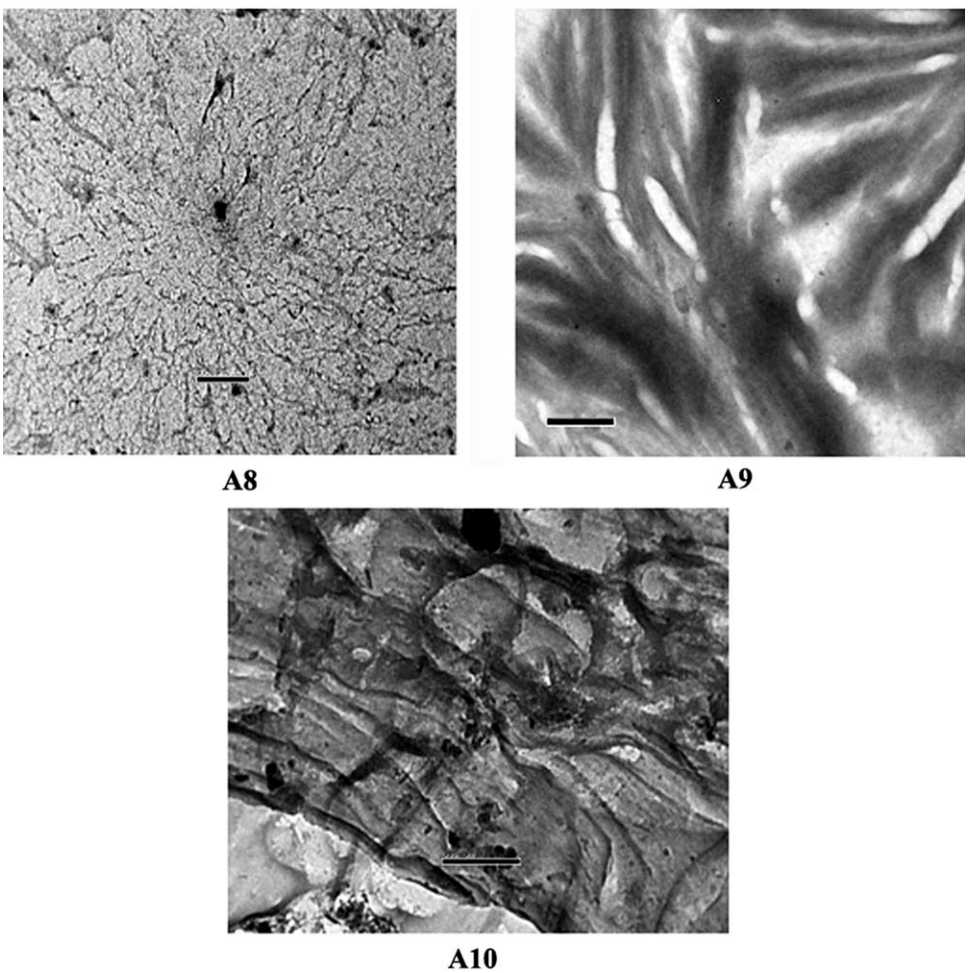

Figure 15 TEM of A_8, A_9, and A_{10} (black bar = 200 nm).

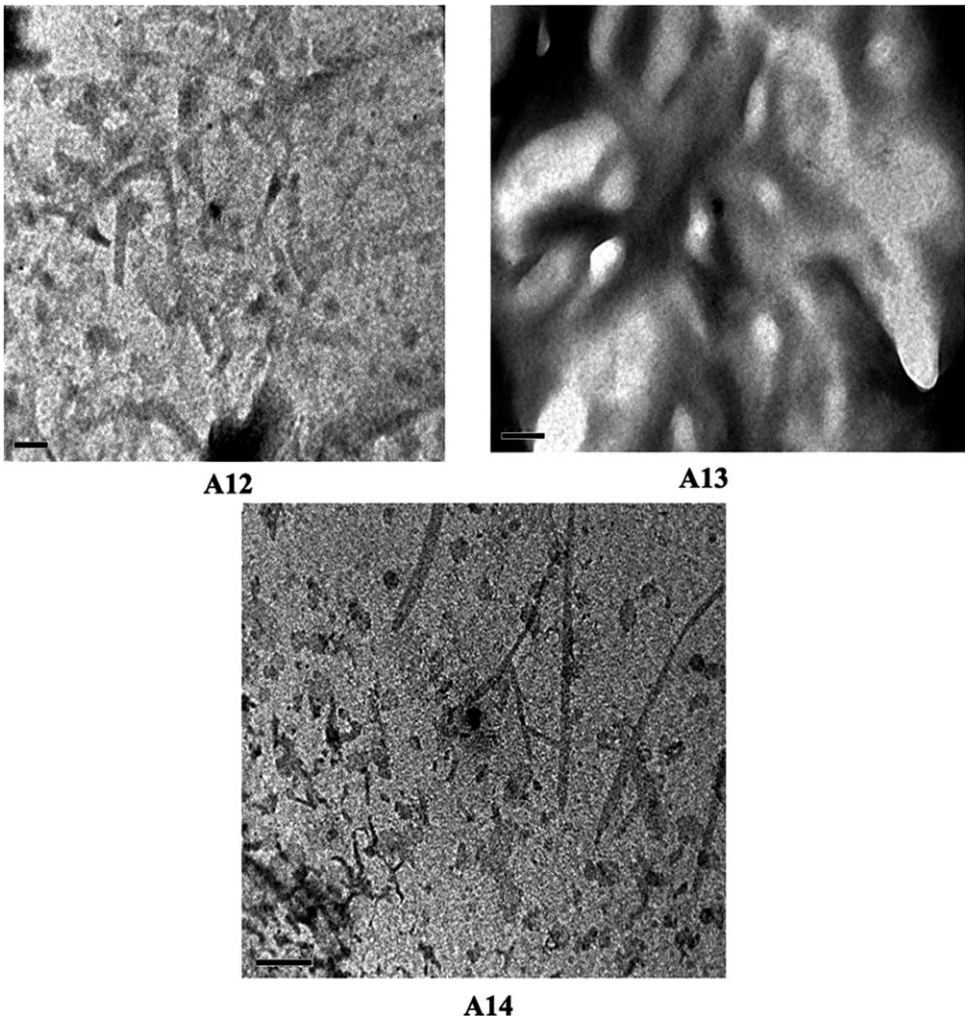

Figure 16 TEM of A_{12}, A_{13}, and A_{14} (black bar = 200 nm).

particles within the polymer matrices. As shown in Figure 16, TEM images of A_{12}, A_{13}, and A_{14} clearly indicate the intercalation of Laponite layers in the Hyp_1, Hyp_2, and Hyp_3 matrices. Generally, TEM showed that the stacks of the intercalated clay platelets and the individual exfoliated platelets were embedded in the polymer matrices. XRD previously obtained results supported the fact of lower intensity of crystal structure in the formed nancomposites in most cases.

CONCLUSIONS

The polyamidoamine hyperbranched polymer (Hyp) managed to form intercalated nanocomposites with both of montmorillonite and laponite. Also, the modified hyperbranched polymers with hydrophobic polymeric ends successfully formed such intercalated nanocomposites. Such clays were used in two loading percents, such as 15 and 4%. Several evidences on the formation of such nanocomposites were provided from XRD, thermal analyses and TEM. Generally, intercalated nanocomposites mostly formed than the exfoliated ones because of the bulkiness of the hyperbranched polymers. However, exfoliation happened only in case of quaternized hyperbranched polymer by using 4% loading percent of montmorillonite and laponite. Generally, these products can be employed as multipurpose masterbatches that can impart different modes of action; rheology modifiers, stabilizing agents against thermal degradation and UV radiation, reinforcing agents or toughners. Furthermore, they may be used as hardeners for thermoset polymers to limit the problems encountered in the industry as a result of the intensive associated shrinkage during curing reactions.

References

1. Ramanathan, T.; Liu, H.; Brinson, L. C. J Polym Sci Part B: Polym Phys 2006, 44, 470.
2. Ajayan, P. M.; Giannaris, C.; Rubio, A. Adv Mater 2000, 12, 750.
3. Burgaz, E.; Lian, H.; Estevez, L.; Giannelis, E. P. Polymer 2009, 50, 2384.

4. Park, C.; Smith, J. J.; Connell, J. W.; Lowther, S. E. Polymer 2005, 46, 9694.
5. Yei, D. R.; Kuo, S. W.; Fu, H. K.; Chang, F. C. Polymer 2005, 46, 741.
6. Adom, K. O.; Guymon, C. A. Polymer 2008, 49, 2636.
7. Yei, D. R.; Kuo, S. W.; Fu, H. K.; Chang, F. C. Polymer 2004, 45, 2633.
8. Kim, M. H.; Lee, J. W.; Lim, J. G.; Park, O. O. J Appl Polym Sci 2004, 92, 2144.
9. Tsai, P. H.; Yang, I. K. Polymer 2006, 47, 5131.
10. Song, M.; Ansarifar, C. W. A.; Richardson, M. Polym Int 2005, 54, 560.
11. Shishan, W.; Dingjun, J.; Xiaodong, O.; Jian, S. Polym Eng Sci 2004, 44, 2070.
12. Fang, Q.; Xiao, L. Polymer 2006, 47, 3049.
13. Charles, U.; Kaiwen, L. Polymer 2006, 47, 2984.
14. Liu, Y. L.; Chang, Y. H.; Liang, M. Polymer 2008, 49, 5405.
15. Milan, A.; Palacio, F.; Serin, V. Polymer 2009, 50, 1088.
16. Alonso, R. H.; Estevez, L.; Giannelis, E. P. Polymer 2009, 50, 2402.
17. Okamoto, M.; Morita, S.; Kotaka, T. Polymer 2001, 42, 2685.
18. Okamoto, M.; Morita, S.; Kotaka, T.; Tateyama, H. Polymer 2001, 42, 1201.
19. Chen, Z.; Huang, C.; Zhang, Y.; Gong, K. J Appl Polym Sci 2000, 75, 796.
20. Noh, M. W.; Lee, D. C. Polym Bull 1999, 42, 619.
21. Fu, X.; Qutubuddin, S. Polymer 2001, 42, 807.
22. Xiao, P.; Xiao, M.; Gong, K. Polymer 2001, 42, 4813.
23. Tseng, C. R.; Wu, J. Y.; Lee, H. Y.; Chang, F. C. Polymer 2001, 42, 10063.
24. Zeng, Q. H.; Wang, D. Z.; Yu, A. B.; Lu, G. Q. Nanotechnology 2002, 13, 549.
25. Friedlander, H. Z.; Frink, C. R. Polym Lett 1964, 2, 475.
26. Gao, D.; Heimann, R. B.; Muhammad, M. J Mater Sci 1999, 34, 1543.
27. Xia, X.; Yih, J.; Hu, Z. Polymer 2003, 44, 3389.
28. Gultek, A.; Seckin, T.; Onal, Y.; Icduygu, G. J Appl Polym Sci 2001, 81, 512.
29. Koo, C. M.; Ham, H. T.; Kim, S. O.; Chung, I. J. Polymer 2003, 44, 681.
30. Parfitt, R. L.; Greenland, D. J. Clay Miner 1970, 8, 305.
31. Hsu, S. L. C.; Chang, K. C. Polymer 2002, 43, 4097.
32. Wu, L.; Cao, D.; Huang, Y.; Li, B. G. Polymer 2008, 49, 742.
33. Bailly, M.; Kontopoulou, M. Polymer 2009, 50, 2472.
34. Morgan, A. B.; Harris, J. D. Polymer 2003, 44, 2313.
35. Kelarakis, A.; Giannelis, E. P.; Yoon, K. Polymer 2007, 48, 7567.
36. Plummer, C. J. G.; Rodlert, M.; Manson, J. A. E. Chem Mater 2002, 14, 486.
37. Bader, S. J.; Parquette, J. R. Tetrahedron 2005, 61, 8329.
38. Peng, H.; Tang, B. Z. Polymer 2005, 46, 5746.
39. Zou, J.; Shi, W. Compos A 2005, 36, 631.
40. Hua, J. L.; Qian, S. X. Polymer 2004, 45, 7143.
41. Boogh, L. Polymer 1999, 40, 2249.
42. Samuelsson, J.; Johansson, M. Prog Org Coat 2004, 50, 193.
43. Gao, C.; Wang, Z. React Funct Polym 2004, 58, 65.
44. Benthem, R. Prog Org Coat 2000, 40, 203.
45. Flory, P. J. J Am Chem Soc 1952, 74, 2718.
46. Gao, C.; Yan, D. Prog Polym Sci 2004, 29, 183.
47. Yates, C. R.; Hayes, W. Eur Polym J 2004, 40, 1257.
48. Tomalia, D. A.; Fre'chet, J. M. J. A. J Polym Sci: Part A: Polym Chem 2002, 40, 2719.
49. Buhleier, E.; Wehner, W.; Vogtle, F. Synthesis 1978, 155.
50. Baskaran, D. Polymer 2003, 44, 2213.
51. Hawker, C. J.; Frechet, J. M. J. J Am Chem Soc 1990, 112, 7638.
52. Webster, O. W.; Kim, Y. H. Macromolecules 1992, 25, 5561.
53. Frechet, J. M. J.; Hawker, C. J. J Am Chem Soc 1991, 113, 4583.
54. Wang, S.; Matyjaszewski, K. Macromolecules 1995, 28, 7901.
55. Haddleton, D.; Hannon, J.; Schooter, J. Macromolecules 1997, 30, 2190.
56. Granel, C.; Dubois, P.; Jerome, R.; Teyssie, P. Macromolecules 1996, 29, 8576.
57. Percec, V.; Barboiu, B. Macromolecules 1995, 28, 7970.
58. Braunecker, W. A.; Matyjaszewski, K. Prog Polym Sci 2007, 32, 93.
59. Matyjaszewski, K.; Pintauer, T. Coord Chem Rev 2005, 249, 1155.
60. Destarac, M.; Boutevin, B. Macromol Rapid Commun 1997, 18, 967.
61. Xia, J.; Matyjaszewski, K. Macromolecules 1997, 30, 7697.
62. Liu, C. H.; Gao, C.; Yan, D. Y. Chem Res Chin 2005, 21, 345.